Exploring the influence of high order transverse modes on the temporal dynamics in an optically pumped mode-locked semiconductor disk laser

C. H. Tsou,[1] H. C. Liang,[2] C. P. Wen,[1] K. W. Su,[1] K. F. Huang,[1] and Y. F. Chen[1,3,*]

[1]*Department of Electrophysics, National Chiao Tung University, 1001 Ta-Hsueh Rd. Hsinchu 30010, Taiwan*
[2]*Institute of Optoelectronic Science, National Taiwan Ocean University, Keelung 20224, Taiwan*
[3]*Department of Electronics Engineering, National Chiao Tung University, 1001 Ta-Hsueh Rd. Hsinchu, Taiwan*
[*]*yfchen@cc.nctu.edu.tw*

Abstract: We quantitatively investigate the influence of high-order transverse modes on the self-mode locking (SML) in an optically pumped semiconductor laser (OPSL) with a nearly hemispherical cavity. A physical aperture is inserted into the cavity to manipulate the excitation of high-order transverse modes. Experimental measurements reveal that the laser is operated in a well-behaved SML state with the existence of the $TEM_{0,0}$ mode and the first high-order transverse mode. While more high-order transverse modes are excited, it is found that the pulse train is modulated by more beating frequencies of transverse modes. The temporal behavior becomes the random dynamics when too many high-order transverse modes are excited. We observe that the temporal trace exhibits an intermittent mode-locked state in the absence of high-order transverse modes.

OCIS codes: (140.5960) Semiconductor lasers; (140.4050) Mode-locked lasers; (140.7270) Vertical emitting lasers.

References and links

1. A. C. Tropper, H. D. Foreman, A. Garnache, K. G. Wilcox, and S. H. Hoogland, "Vertical-external-cavity semiconductor lasers," J. Phys. D Appl. Phys. **37**(9), R75–R85 (2004).
2. M. Kuznetsov, F. Hakimi, R. Sprague, and A. Mooradian, "High-power (>0.5-W CW) diode-pumped vertical-external-cavity surface-emitting semiconductor lasers with circular TEM_{00} beams," IEEE Photon. Technol. Lett. **9**(8), 1063–1065 (1997).
3. B. Heinen, T.-L. Wang, M. Sparenberg, A. Weber, B. Kunert, J. Hader, S. W. Koch, J. V. Moloney, M. Koch, and W. Stolz, "106 W continuous-wave output power from vertical-external-cavity surface-emitting laser," Electron. Lett. **48**(9), 516–517 (2012).
4. U. Keller and A. C. Tropper, "Passively modelocked surface-emitting semiconductor lasers," Phys. Rep. **429**(2), 67–120 (2006).
5. H. Haus, "Mode-locking of lasers," IEEE J. Sel. Top. Quantum Electron. **6**(6), 1173–1185 (2000).
6. Y. F. Chen, Y. C. Lee, H. C. Liang, K. Y. Lin, K. W. Su, and K. F. Huang, "Femtosecond high-power spontaneous mode-locked operation in vertical-external cavity surface-emitting laser with gigahertz oscillation," Opt. Lett. **36**(23), 4581–4583 (2011).
7. H. C. Liang, Y. C. Lee, J. C. Tung, K. W. Su, K. F. Huang, and Y. F. Chen, "Exploring the spatio-temporal dynamics of an optically pumped semiconductor laser with intracavity second harmonic generation," Opt. Lett. **37**(22), 4609–4611 (2012).
8. L. Kornaszewski, G. Maker, G. P. A. Malcolm, M. Butkus, E. U. Rafailov, and C. J. Hamilton, "SESAM-free mode-locked semiconductor disk laser," Laser Photon. Rev. **6**(6), L20–L23 (2012).
9. A. R. Albrecht, Y. Wang, M. Ghasemkhani, D. V. Seletskiy, J. G. Cederberg, and M. Sheik-Bahae, "Exploring ultrafast negative Kerr effect for mode-locking vertical external-cavity surface-emitting lasers," Opt. Express **21**(23), 28801–28808 (2013).
10. M. Gaafar, D. A. Nakdali, C. Möller, K. A. Fedorova, M. Wichmann, M. K. Shakfa, F. Zhang, A. Rahimi-Iman, E. U. Rafailov, and M. Koch, "Self-mode-locked quantum-dot vertical-external-cavity surface-emitting laser," Opt. Lett. **39**(15), 4623–4626 (2014).
11. H. C. Liang, C. H. Tsou, Y. C. Lee, K. F. Huang, and Y. F. Chen, "Observation of self-mode-locking assisted by high-order transverse modes in optically pumped semiconductor lasers," Laser Phys. Lett. **11**(10), 105803 (2014).
12. M. Gaafar, P. Richter, H. Keskin, C. Möller, M. Wichmann, W. Stolz, A. Rahimi-Iman, and M. Koch, "Self-mode-locking semiconductor disk laser," Opt. Express **22**(23), 28390–28399 (2014).

13. N. Hodgson and H. Weber, "Measurement of Beam Quality," in *Laser Resonators and Beam Propagation Fundamentals, Advanced Concepts and Applications*, 2nd ed. (Springer, 2005), pp. 713–715.

1. Introduction

Nowadays, optically pumped semiconductor lasers (OPSLs), so called vertical external cavity surface emitting lasers (VECSELs), have become versatile light sources with advantages including high output power, flexible emission wavelength, and nearly diffraction-limited beam quality [1]. Since the first demonstration by M. Kuznetsov *et al* [2], OPSLs have been extensively explored for various emission schemes. In addition to high power continuous-wave (CW) emission [3], methods of generating short pulses in OPSLs are also aroused considerable interest, such as mode-locked operation [4].

The laser operated in mode-locked state is a well-known technique to produce pulses with the pulse duration on the order of picoseconds or femtoseconds [5]. Among numerous mode-locked methods, the phenomenon of self-mode-locking (SML) is of greatly scientific interest in a laser resonator. Here, SML means that no additional active or passive mode-locking elements (such as saturable absorbers) are used in the laser cavity except for the gain medium. In recent years, the SML operation has been reported in OPSLs with different cavity configurations [6–12]. One of these works experimentally explored that the high-order transverse mode played an important role in achieving the SML operation [11]. The experimental results implied that the phase locking between lasing longitudinal modes can be assisted by the existence of $TEM_{1,0}$ mode. On the other hand, M. Gaafar *et al* demonstrated an excellent beam quality of a VECSEL operated in SML state with fundamental transverse mode [12]. So far, the physical mechanism of SML operation in OPSLs is still ambiguous. There is a controversial issue whether SML operation can be assisted by high-order transverse modes in OPSLs. However, the influence of high-order transverse modes on SML operation in an OPSL has not been quantitatively analyzed yet.

With inserting a physical aperture into the cavity, the excitation of high-order transverse modes can be dominated by the aperture size. In this paper, we explore the performance of SML in an OPSL with a nearly hemispherical cavity by utilizing different aperture sizes to manipulate the excitation of high-order transverse modes. At first, we numerically calculate the energy of high-order transverse modes within the aperture size to analyze the excitation of high-order transverse modes. Based on the calculated results, we systematically measure the temporal dynamics of the laser output with specific aperture sizes. With the appropriate aperture size, the experimental observations reveal that only $TEM_{0,0}$ mode and the first high-order transverse mode are excited in the laser cavity. Meanwhile, a well-behaved mode-locked pulse train is experimentally observed. When more high-order transverse modes are excited with using a larger aperture size, the mode-locked pulse train is found to be modulated with the transverse beat frequency. Furthermore, in the absence of the aperture, the temporal behavior becomes the random dynamics because there are too many beating frequencies of transverse modes. On the other hand, when the aperture size is too small to excite high-order transverse modes, we observe that the laser is operated in an intermittent mode-locked state.

2. Cavity configuration and design of aperture size

Figure 1(a) illustrates the schematic of the laser experiment. The laser cavity consists of a concave mirror, a semiconductor gain chip, a pump laser diode, and an aperture. The gain chip and the pump laser diode were obtained from a commercial OPSL module (Coherent Inc.). The active region was a structure of multiple quantum wells to form a resonant periodic gain.

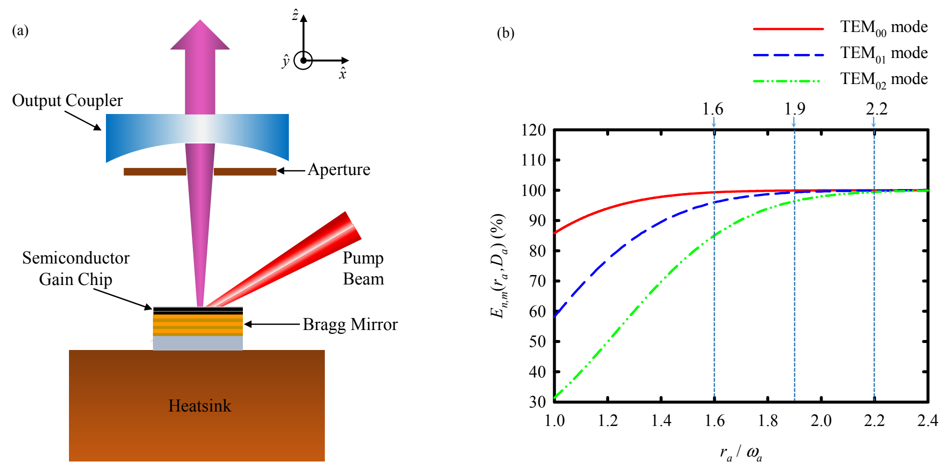

Fig. 1. (a) Schematic diagram of the experimental setup for exploring the SML in an OPSL. (b) Calculated results for the energy of high-order transverse modes within the aperture $E_{n,m}(r_a, D_a)$ versus the ratio of apertures size to the cavity mode size on the aperture r_a/ω_a.

To form a front mirror, the gain chip included a structure of distributed Bragg reflectors (DBRs). The photoluminescence emission wavelength of the gain chip was approximately 1060 nm at room temperature. The gain chip was soldered with indium to chemical vapor deposition diamond heat spreader with DBR side down for effectively removing the heat from the gain structure. The gain structure was antireflection coated at the wavelengths of 808 nm and 1060 nm. The radius of the 808 nm pump beam ω_p was approximately 320 µm. The concave output coupler was utilized with the radius of curvature R_{oc} of 100 mm and the output transmission of 2%. In order to excite high-order transverse modes effortlessly, a nearly hemispherical cavity was designed with the cavity length L_{cav} of 96 mm. With ABCD matrix, the basic formula of cavity mode size is given by [13]:

$$\omega(z) = \omega_0 \sqrt{\left[1 + \left(M^2 z/z_R\right)^2\right]}, \tag{1}$$

where ω_0 is the beam waist, $\omega_0^2 = \lambda z_R/\pi$, $z_R = \sqrt{L_{cav}\left(R_{oc} - L_{cav}\right)}$, λ is the emission wavelength, and M^2 is the beam propagation factor. With the coordinates shown in Fig. 1(a), the beam propagation factor M^2 for a Hermite-Gaussian transverse mode, related to $TEM_{n,m}$, is ($2n$ + 1) in the x- direction and ($2m$ + 1) in the y- direction. In this nearly hemispherical cavity, the beam waist was the cavity mode size on the gain chip, and was calculated to be 81 μm. Hence, the pump-to-mode size ratio was obtained to be 3.95. This large value of the pump-to-mode size ratio caused the pump thresholds of high-order transverse modes to be extremely low [11]. This nearly hemispherical cavity was employed for generating lots of high-order transverse modes. With inserting a physical aperture into the cavity, the excitation of high-order transverse modes could be manipulated. The distance between the aperture and the output coupler D_a was set to be 5 mm. With Eq. (1), the cavity mode size of fundamental transverse mode at the position of the aperture ω_a was approximately 386 μm.

To analyze the influence of aperture size on the excitation of high-order transverse modes, we numerically calculate the energy of high-order transverse modes within the aperture area. With the coordinates shown in Fig. 1(a), the electric field in the laser cavity can be expressed as

$$\psi_{n,m,l}^{(HG)}\left(x,y,z\right) = \sqrt{2/L_{cav}}\,\Phi_{n,m}\left(x,y,z\right)\times\sin\left[k_{n,m,l}\tilde{z} - \left(m+n+1\right)\tan^{-1}\left(z/z_R\right)\right], \tag{2}$$

where

$$\Phi_{n,m}(x,y,z)=\frac{1}{\sqrt{2^{n+m-1}\pi n!m!}}\frac{1}{\omega(z)}H_n\left[\frac{\sqrt{2}x}{\omega(z)}\right]H_m\left[\frac{\sqrt{2}y}{\omega(z)}\right]e^{-\frac{2(x^2+y^2)}{\omega^2(z)}}, \tag{3}$$

$H_n(\bullet)$ is the Hermite polynomials of order n, $\tilde{z}=z+\left[\left(x^2+y^2\right)z\right]/\left[2\left(z^2+z_R^2\right)\right]$, $k_{n,m,l}=2\pi f_{n,m,l}/c$, $f_{n,m,l}$ is the eigenmode frequency, c is the speed of light in vacuum, l is the longitudinal mode index, and n and m are the transverse mode indices. The eigenmode frequency can be expressed as $f_{n,m,l}=\left[l\Delta f_L+(n+m+1)\Delta f_T\right]$ where Δf_L is the longitudinal mode spacing and Δf_T is the transverse mode spacing. For the plano-concave cavity, the transverse mode spacing Δf_T is given by $\Delta f_T=\Delta f_L\left[(1/\pi)\tan^{-1}\left(L_{cav}^*/R_{oc}\right)\right]$, where $\Delta f_L=c/2L_{cav}^*$ and L_{cav}^* is the optical cavity length. In our cavity configuration, the values of Δf_L and Δf_T was calculated to be 1.56 GHz and 687 MHz, respectively. Considering the central emission wavelength, the energy of transverse modes within the aperture area can be expressed as a definite integral of $\left|\psi_{n,m,l=0}^{(HG)}(x,y,z)\right|^2$:

$$E_{n,m}(r_a,z)=\int_0^{r_a}\int_0^{\sqrt{r_a^2-y^2}}\left|\psi_{n,m,l=0}^{(HG)}(x,y,z)\right|^2 dxdy, \tag{4}$$

where r_a is the radius of aperture. Figure 1(b) depicts $E_{n,m}(r_a,D_a)$ of $TEM_{0,0}$, $TEM_{0,1}$, and $TEM_{0,2}$ modes versus the ratio of r_a to ω_a. When the value of r_a/ω_a is larger than 2.2, each energy of $TEM_{0,0}$, $TEM_{0,1}$, and $TEM_{0,2}$ modes within the aperture remains the total energy. It reveals that the aperture sizes in this region cannot affect the excitation of $TEM_{0,0}$, $TEM_{0,1}$, and $TEM_{0,2}$ modes. In the range of $2.2\geq r_a/\omega_a\geq 1.9$, the energy of $TEM_{0,2}$ mode within the aperture becomes to reduce with the decreasing aperture size. Thus, the pump threshold of $TEM_{0,2}$ mode can be increased when the value of r_a/ω_a is less than 2.2. In the range of $1.9\geq r_a/\omega_a\geq 1.6$, $E_{0,1}(r_a,D_a)$ and $E_{0,2}(r_a,D_a)$ both decline with the decreasing aperture size, but the energy of $TEM_{0,0}$ mode within the aperture still remains the total energy. It implies that the pump thresholds of $TEM_{0,1}$, and $TEM_{0,2}$ modes can be both risen with aperture sizes in the range of $1.9\geq r_a/\omega_a\geq 1.6$. While the value of r_a/ω_a is less than 1.6, it can be seen that each energy of transverse modes cannot maintain the total energy. In addition to the increasing pump thresholds of $TEM_{0,1}$ and $TEM_{0,2}$ modes, the lasing threshold may be also risen. Based on the calculated results, we can manipulate the excitation of high-order transverse modes with the different aperture sizes. Consequently, the radii of aperture in experiments were 0.875, 0.75, 0.625, and 0.5 mm corresponding to r_a/ω_a of 2.267, 1.943, 1.619 and 1.295, respectively.

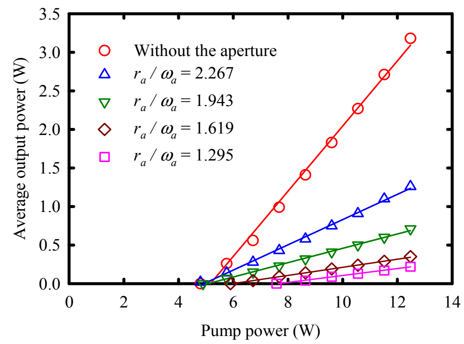

Fig. 2. Average output power versus pump power with different values of r_a/ω_a .

3. Experimental results and discussion

First of all, we explore the influence of the aperture size on the output power. Figure 2 depicts the average output power versus the pump power with different aperture sizes. In the absence of the aperture, the average output power was 3.18 W at a pump power of 12.48 W, and the slope efficiency was approximately 43.45%. With the decreasing aperture size, the maximum output powers were 1.26, 0.71, 0.35, and 0.22 W with r_a/ω_a = 2.267, 1.943, 1.619 and 1.295, respectively. The drop of the maximum output power with r_a/ω_a = 2.267 indicated that there were lots of high-order transverse modes in addition to $TEM_{0,0}$, $TEM_{0,1}$, and $TEM_{0,2}$ modes in the output beam. Thus, the significant reducing of the output power with the decreasing aperture size was caused by the suppression of high-order transverse modes.

Figure 3 shows the overall observations for the laser operated at a pump power of 7.68 W in the absence of the aperture. The temporal behavior of the laser output was detected by a high-speed InGaAs photodetector (Electro-Optics Technology Inc. ET-3500 with rise time 35 ps), whose output signal was connected to a digital oscilloscope (Lecroy 820Zi-A) with 20 GHz electrical bandwidth and a sampling interval of 25 ps. As shown in Fig. 3(a), the temporal behavior displayed the random dynamics instead of a mode-locked pulse train. It was found that the laser was not operated in a SML state when the aperture was not inserted into this nearly hemispherical cavity. The output signal of the photodetector was also delivered to a radio frequency (RF) spectrum analyzer (Agilent 8563EC) with the bandwidth of 26.5 GHz. In Fig. 3(b), there were a lot of frequency peaks in the RF spectrum in addition to the harmonics of the longitudinal mode spacing Δf_L = 1.567 GHz, and the peak values were generally less than 30 dB. The results revealed that there were many beating frequencies of transverse modes in the RF spectrum. As plotted in the inset of Fig. 3(b), the transverse pattern of the output beam displayed distinctly elliptical shape which was consisted of many high-order transverse modes. Consequently, the temporal behavior displayed the random dynamics with too many beating frequencies of transverse modes.

Next, we inserted the physical aperture into the cavity and set the value of r_a/ω_a to 2.267. The performance of SML was observed for the laser operated at the same pump power. As shown in Fig. 4(a), the temporal trace displayed an indistinctly mode-locked pulse train on top of a CW background. Besides, the mode-locked pulse train was modulated with the additional envelope caused by a beating frequency. Referring to Fig. 4(b), the beating frequency was measured to be approximately 186 MHz which was corresponded to $\Delta f_L - 2\Delta f_T$. All frequency peaks in the RF spectrum were measured at the frequencies of $f = q \cdot \Delta f_L \pm p \cdot \Delta f_T$ where q and p were integers. These frequency peaks represented that the first and second high-order transverse modes were excited in the output beam at least. The peak values were generally less than 30 dB which was consistent with the indistinctly mode-

#239896 - $15.00 USD Received 27 Apr 2015; revised 4 Jun 2015; accepted 4 Jun 2015; published 11 Jun 2015

locked pulse train. As plotted in the inset of Fig. 4(b), the transverse pattern which was not a Gaussian-like distribution. The results revealed that laser output did not operated in a well-behaved SML state with the existence of the first and second high-order transverse modes.

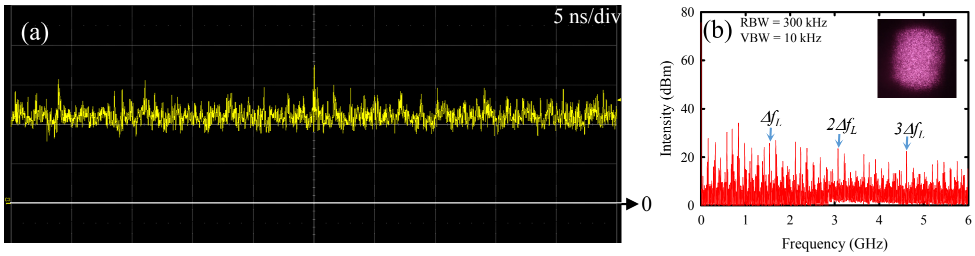

Fig. 3. Experimental measurements for overall performances in the absence of the aperture: (a) temporal trace, (b) RF power spectrum. Inset: transverse pattern.

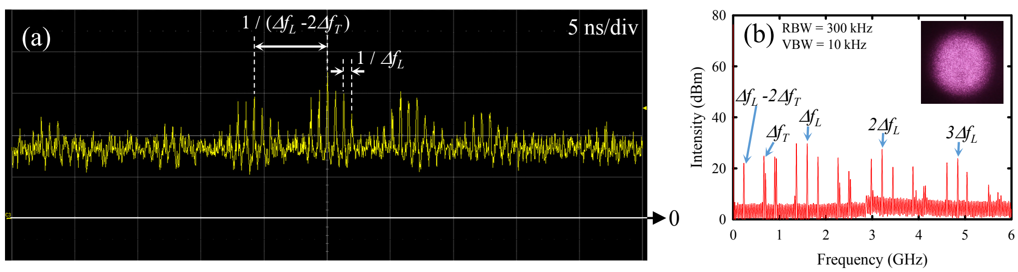

Fig. 4. Experimental measurements with $r_a/\omega_a = 2.267$: (a) temporal trace, (b) RF power spectrum. Inset: transverse pattern.

When the value of r_a/ω_a was reduced to 1.943, we explored that the laser was operated in a long-lasting SML state. The critical pump power for achieving SML operation was experimentally found to be 7.11 W. The experimental results of the SML state was measured at a pump power of 7.68 W. The pump power range for the long-lasting SML state was from 7.11 W to 10.56 W. Figures 5(a) and 5(b) show the temporal traces on two different time scales, one with the time span of 200 μs demonstrating the amplitude stability, the other with the time span of 50 ns demonstrating mode-locked pulses. The full modulation of pulse trains without any CW background indicates the realization of complete mode locking, although some slight amplitude fluctuation which was caused by the group velocity dispersion existed in the long span pulse train. In Fig. 5(c), the peak values of the harmonics of the longitudinal modes spacing in the RF spectrum were increased significantly, and the signal to noise was approximately 60 dB, regarding as larger than the standard value of well-behaved SML operation. In the meantime, there were two beat peaks which accompanied the harmonics of the longitudinal mode spacing in the RF spectrum. The beat frequency was measured to be 687 MHz which was corresponded to the transverse mode spacing Δf_T. The peak values of beat frequencies were less than 25 dB. The appearance of the beat peaks at the frequencies of $f = u \cdot \Delta f_L \pm \Delta f_T$ with u = 1, 2, 3, 4, 5, 6 in the RF spectrum distinctly revealed the existence of the first high-order transverse mode.

#239896 - $15.00 USD Received 27 Apr 2015; revised 4 Jun 2015; accepted 4 Jun 2015; published 11 Jun 2015

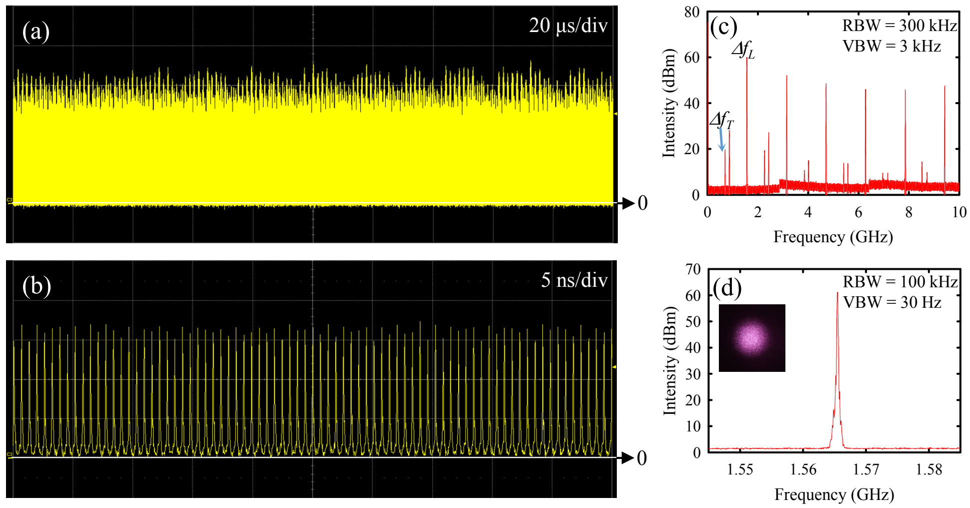

Fig. 5. Experimental measurements for overall performances of the laser operated in the mode-locked state with $r_a/\omega_a = 1.943$: (a) oscilloscope trace with the time span of 200 µs, (b) oscilloscope trace with the time span of 50 ns, (c) RF spectrum with the frequency span of 10 GHz, (d) RF spectrum of the fundamental harmonic with the frequency span of 40 MHz. Inset: transverse pattern.

Figure 5(d) illustrates the RF spectrum of the fundamental harmonic. The full width at half maximum (FWHM) of the fundamental harmonic was measured to be approximately 400 kHz which implies a nice long term stability. In the inset of Fig. 5(d), the transverse pattern was slightly elliptical. Note that the temporal traces in the position out of the beam center were generally found to be modulated with the transverse beat frequency. This spatiotemporal dynamics is attributed to the simultaneous longitudinal and transverse mode locking [7].

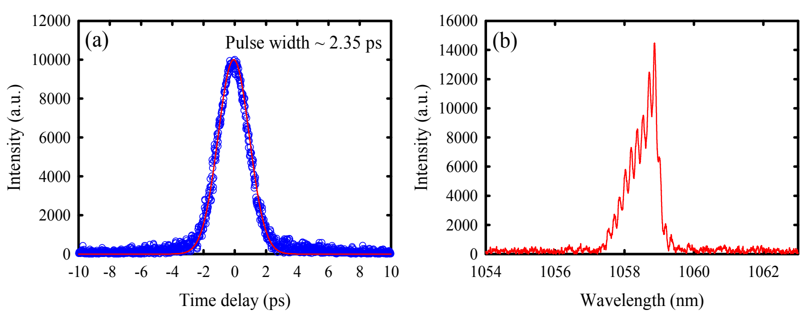

Fig. 6. Experimental results of (a) auto-correlation trace and (b) optical spectrum in the SML state.

The pulse width was measured with a commercial autocorrelator (APE Pulse Check, Angewandte Physik and Elektronik GmbH). Figure 6(a) depicts the FWHM of the central peak of the second-order autocorrelation trace. Assuming the temporal intensity to be a Gaussian-shaped profile, the pulse width was approximately 2.35 ps. A Fourier optical spectrum analyzer (Advantest Q8347), which was constructed with a Michelson interferometer, was employed to monitor the spectral information with the resolution of 0.003 nm. As shown in Fig. 6(b), the FWHM in the optical spectrum was found to be as wide as 0.78 nm. Therefore, the time–bandwidth product of the mode-locked pulse was approximately 0.491, which was 1.1 times the Fourier-limited value of 0.441. The slightly periodic modulation in the optical spectrum was caused by the etalon effect induced by the output coupler. The spacing between two periodic peaks was measured to be 0.15 nm which was corresponded to the optical length of the output coupler of 3.73 mm. When the value of r_a/ω_a was decreased to 1.619, the performance of SML was as great as the case of $r_a/\omega_a = 1.943$. For the case of $r_a/\omega_a = 1.619$, the critical pump power for achieving self-mode-locked state was measure to be 7.49 W which was slightly higher than the case of $r_a/\omega_a = 1.943$. The pump power range of self-mode-locked state was from 7.49 W to 10.56 W. The results signify that a long-lasting SML operation can be achieved when only $TEM_{0,0}$ mode and the first high-order transverse mode are excited in the laser cavity.

Finally, it was found that the laser was operated in an intermittent mode-locked state when the value of r_a/ω_a decreased to 1.295. In Fig. 7(a), the long-span temporal trace of the laser output is shown for a time window of 200 μs. It can be obviously seen that the temporal behaviors were quite different between the region A and the region B. The short-span temporal traces of region A and B are illustrated in Fig. 7(b) and 7(c) for a time window of 50 ns, respectively. Referring to Fig. 7(b), a mode-locked pulse train can be observed though the performance was not as good as the case shown in Fig. 5. The temporal trace of region B displayed an irregular signal on top of a CW background, as depicted in Fig. 7(c). The results of temporal dynamics indicated that the laser output did not exhibit a long-lasting mode-locked pulse train. In Fig. 7(d), there were only the harmonics of the longitudinal mode spacing in the RF spectrum. The peak values in the RF spectrum were generally less than 25 dB, considering less than the standard value of well-behaved mode-locked lasers. In Fig. 7(e), the transverse pattern was more circularly symmetric than the beam profile shown in Fig. 5. According to the results in the RF spectrum and the transverse pattern, it could be verified that there was only fundamental transverse mode in the output beam. Consequently, the experimental measurements indicate that the laser can be operated in an intermittent mode-locked state when the aperture size is too small to excite high-order transverse modes.

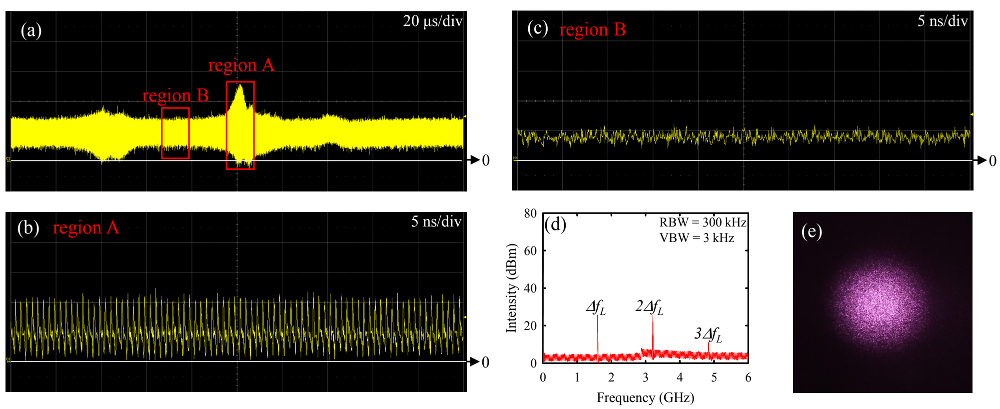

Fig. 7. Experimental measurements for overall performances of the laser operated in intermittent mode-locked state with $r_a/\omega_a = 1.295$: (a) long-span temporal trace, (b) short-span temporal trace for region A, (c) short-span temporal trace for region B, (d) RF power spectrum, (e) transverse pattern.

4. Conclusions

In summary, we have quantitatively explored the influence of high-order transverse modes on SML in an OPSL with a nearly hemispherical cavity. We have employed the different aperture sizes to control the excitation of high-order transverse modes. To analyze the excitation of high-order transverse modes, we have numerically calculated the energy of high-order transverse modes within the aperture area. According to the calculated results, specific aperture sizes have been exploited to observe the influence of high-order transverse modes on the temporal dynamics. Experimental results have indicated that the SML operation can be achieved with the appropriate aperture size which only allows the existence of fundamental transverse mode and the first high-order transverse mode. We have demonstrated that the pulse train is modulated with the transverse beat frequency when we use the larger aperture size to excite more high-order transverse modes. Moreover, the random dynamics of the laser output has been observed while there are too many beating frequencies of transverse modes. Eventually, it has been found that the laser is operated in an intermittent mode-locked state when the aperture size is too small to permit the excitation of high-order transverse modes.

Acknowledgments

The authors acknowledge the Ministry of Science and Technology for the financial support of this research under Contract No. MOST 103-2112-M-009-0016-MY3.